PREPARATION AND STRUCTURAL CHARACTERIZATION OF
β – TCP/PVA NANOPOWDERS

J. Ady[1,2*], S. Meliana[1], S.F. Umroati[1], S.D.A. Ariska[1], D.I. Rudyardjo[1,2], Siswanto[1,2],

A.A. Nurpratiwi[3]

[1]Department of Physics, Faculty of Science and Technology, Airlangga University, 60115 Surabaya, Indonesia

[2]Biomedical Engineering Study Program, Faculty of Science and Technology, Airlangga University, 60115

Surabaya, Indonesia

[3]Department of Materials Science and Engineering, National Cheng Kung University, No. 1 University Road,

East District 701, Tainan City, Taiwan

*e-mail: jan-a@fst.unair.ac.id

Abstract. The research of β-Tricalcium phosphate (β-TCP) nanopowders without and with polyvinyl alcohol (PVA) effect have been prepared by the sol-gel technique. The crystallography characteristic has been confirmed by revealed the relevant parameter for 0.0 wt%, 1.0 wt%, 2.0 wt%, and 4.0 wt% of PVA while conducted at 800 $^{\circ}$C. Where its values are determined from the parameter of the crystallite size, crystallite strain, crystallite dislocation, crystallinity, and the preferential plane crystallographic using the XRD result. Whilst the morphology is confirmed by the surface topography image and the atomic ratio of Ca/P using the SEM-EDX result. Eventually, its thermal response is confirmed by the melting point, specific heat capacity, fusion, and crystallization enthalpies parameters, using the DSC-TG using.
Keywords: research, tricalcium phosphate, sol-gel, polyvinyl alcohol, nanopowder, crystallography

1. Introduction

Tribasic calcium phosphate is sometimes abbreviated with TCP and this kind of calcium salt of phosphoric acid with a chemical formula $Ca_3(PO_4)_2$. There are three groups, α-, α'-, and β-TCP as crystalline polymorph. They are potentially used in medicine for bone substitutes either in the form of dense or porous [1]. The α- and α'-TCP characteristics have been found at higher temperatures rather than β-TCP. The α-TCP characteristic is designed as a monoclinic structure at high temperatures and becomes a metastable structure at room temperature. While the α'- characteristic is designed as a hexagonal structure at high temperature. On the contrary, β-TCP is designed as a rhombohedral structure in low temperatures [2-4]. The synthesis of pure TCP powders is not so much reported in the literature compared with hydroxyapatite (HA), as reviewed by Destainville et all [1] and Elliot [5], it can be performed by using either high-temperature solid-state reaction or wet preparation methods at low temperatures. The main problem encountered with both methods is the variability of the powder composition. The solid-state reactions at high temperatures are hardly usable for the synthesis of great quantities because it is difficult to control intimate mixtures of the reagent powders from the complete reaction between them. Therefore, the preparation of stoichiometric final products without residual calcium/phosphorous molar ratio

of the initial precipitate. Whilst, the wet precipitation method cannot be synthesized directly, such as in the β-TCP formation [6-7]. However, the wet precipitation method is simple in the preparation or synthesis, if that is compared to the solid-state reaction.

This work focused on the wet method by way of the sol-gel preparation for β-TCP nanopowders acquire with polyvinyl alcohol (PVA) effect as an advantage additive. The PVA using in this prepared to assist the formation of crystallite with smaller size and this could be removed at the final stage by temperature treatment [8]. In other words, this PVA uses like a catalyzer in the sol-gel preparation technique. The sol-gel method was used in many powder materials preparation due to simplicity in the process and always produce a fine powder with small a size [9-11]. Therefore, this way has been used to found the characteristics of β-TCP nanopowders without or with PVA effect through its study of crystallography, morphology, and thermal behavior with tracking the parameter values of the crystallite size, crystallite strain, crystallite dislocation, crystallographic plane orientation, crystallinity, topographic, the atomic ratio of Ca/P, specific heat capacity, enthalpy of melting, and crystallization.

2. Experimental

Calcium hydroxide and phosphoric acid are used as a precursor for made β-TCP nanopowders without or with PVA effect by the sol-gel preparation method [12-13]. Previously, its calcium oxide is made from calcium carbonate (β-$CaCO_3$) powder by way of sintered that at 900^oC. Subsequently, its reaction with water has found a calcium hydroxide and then dissolves with ethanol for 1.8 M of the calcium hydroxide and added by 1.0 wt%, 2.0 wt%, and 4.0 wt% of PVA. The phosphoric acid solution for 1.2 M was prepared and then added into the previous solution that consists of calcium hydroxide, ethanol, and PVA, as part of the hydrolysis and condensation steps [14-17]. The next step is gel aging until 24 hours at room temperature to reduce its water and its volatility from the gel. The thermal response was examined using the DSC. This looking the effective temperature for β-TCP nanopowders dry form is made through its parameters determined in the fusion and crystallization enthalpies, melting point, and specific heat capacity parameters. The last steps in the sol-gel process are drying and heating, which drying has been conducted for 14 hours at 80^oC and heating for four hours at 800^oC. The PVA type is used here by Sima-Aldrich product with powder form and it has a molecular weight of about $M_w \sim 89.000 – 98.000$. Meanwhile, the XRD equipment is used for data analysis, namely PHILIPS binary(scan) (RD) with anode material Cu-K-Alpha ($\lambda \sim 1.54060$ A^o). The DSC-TG equipment by METTLER TOLEDO product with 120 thermocouples is used for the thermal response of sample and the Pisma ESEM with specification resolution about 3.0 nm at 30 kV in high vacuum is used to morphology test.

Finally, the β-TCP nanopowder dry formed and then is confirmed by several interesting parameters such as crystallite size, crystallite strain, crystallite dislocation, crystallographic plane orientation, crystallinity, using the XRD. Moreover, the surface morphology and its atomic ratio of calcium and phosphorus have been studied by using SEM-EDX.

3. Results and Discussions

There are several results and information of the β-TCP nanopowders without and with 1.0 wt%, 2.0 wt%, 4.0 wt% of PVA effect by looking for the parameter values of crystallite size, crystallite strain, crystallite dislocation, crystallinity, and the preferential crystallographic plane orientation, which all tracked by using the XRD result. DSC-TG results had given information about thermal responses and then are calculated the melting point, fusion and crystallization enthalpies, specific heat capacity, and weight loss parameters. The SEM–EXD result has confirmed information of β-TCP nanopowders morphology through its surface topographic images and Ca/P ratio determined after conducted at 800^oC.

XRD results and discussion. In 1918, P. Scherrer showed that, when parallel monochromatic radiation falls on an oriented random mass of crystals, the diffracted beam is broadened when the particle size is small [18]. The approximation method by the Scherrer equation, such as in Eq. (1) is related to the width of the powder diffraction peak average on crystallite in the polycrystalline powder [19].

$$D = \frac{K\lambda}{\beta \cos\theta},$$
(1)

where D is the average thickness parameter of the crystal in a normal direction to the *hkl* diffracting plane or the crystallite size variable from the Scherrer equation form, K is numerical constant near unity, λ is the wave-length of the incident X-ray, β is the crystallite size contribution to the peak width, and θ is the Bragg angle or peak position in radians. Sample-induced peak broadening is a convolution effect caused by crystallite size and stress. The total sample broadening is usually approximated as a sum of the terms expressed [20-21] in Eq. (2) and (3).

$$\beta_t = \beta_D + \beta_\varepsilon,$$
(2)

or

$$\beta_t = \frac{K\lambda}{D\cos\theta} + 4\varepsilon\tan\theta \cdot$$
(3)

In other words, the variable of the β_D and β_ε becomes equal with Eq. (4) and (5). Respectively, β, β_D, and β_ε are the total broadening, broadening due to crystallite size, and the broadening due to crystallite strain.

$$\beta_D = \frac{K\lambda}{D\cos\theta},$$
(4)

$$\beta_\varepsilon = 4\varepsilon\tan\theta.$$
(5)

Multiplication each side of the Eq. (3) with $cos\theta$ and yield the Eq. (6).

$$\beta_t \cos\theta = 4\varepsilon\sin\theta + \frac{K\lambda}{D}.$$
(6)

Finally, Eq. (6) represents a straight line, in which ε is the gradient or slope of the line and $K\lambda/D$ is the intercept of the straight-line curve. Meanwhile, the crystallite dislocation or dislocation density is defined as a length of dislocation lines per unit volume of the crystal and calculated by the Williamson-Hall relation, as well as shown in Eq. (7). Where dislocation density δ is determined by using the XRD results and based on the broadening of the diffraction lines [22-23].

$$\delta = \frac{1}{D^2}.$$
(7)

The first data analysis is used to define the lattice plane of all samples of β-TCP nanopowders without and with 1.0 wt%, 2.0 wt%, 4.0 wt% of the PVA effect. Previously, by using Bragg's law [19] such as expressed in Eq. (8) and on the first peak (n=1), where n is diffraction order, such as expressed in Eq. (9).

$$2\left(d_{hkl}\right)\sin\theta = n\lambda,$$
(8)

or

$$d_{hkl} = \frac{(n=1)\lambda}{2\sin\theta} = \frac{\lambda}{2\sin\theta}.$$
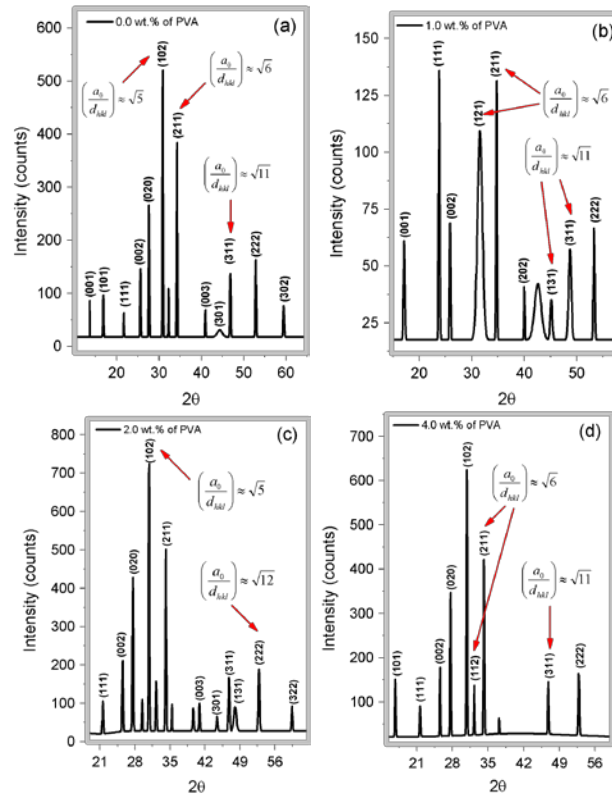(9)

Fig. 1. X-ray diffraction patterns for β-TCP/PVA nanopowder with the Gaussian fit method and Miller indices (hkl); (a) 0.0 wt.%, (b) 1.0 wt.%, (c) 2.0 wt.%, and (d) 4.0 wt.% of PVA

This Eq. (9) gives a value for the lattice spacing d and if this is the first diffraction peak then it was known the type of the crystalline structure of all samples of β-TCP nanopowders without and with 1.0 wt%, 2.0 wt%, 4.0 wt% of PVA effect. The X-ray diffraction pattern yields of these samples already smoothed or fitted by using the Gaussian method, as well as show all results in Fig. 1. These results have been measured and also define as a face-centered cubic (fcc) or cubic close-packed (ccp) unit cell structure for all samples [19-20]. In crystallography, this fcc or ccp that has two indicates the lattice system of crystal, namely are rhombohedral and hexagonal. However, this result was found and define the Miller indices d_{hkl} of lattice plane of β-TCP nanopowders without and with 1.0 wt%, 2.0 wt%, 4.0 wt% of PVA effect have three equal axes a_0 (constant). Therefore, this yield tends to describe a rhombohedral lattice system by fcc or ccp unit cell structure in the ratio formulation of lattice constant and Miller indices, such as shown in Eq. (10).

$$\left(\frac{a_0}{d_{hkl}}\right) = \sqrt{h^2 + k^2 + l^2}. \tag{10}$$

The specific position of XRD patterns of β-TCP nanopowders without and with 1.0 wt%, 2.0 wt%, 4.0 wt% of PVA effect are plotted together in Fig. 2. By using the Gaussian fit method [24]. The preferential crystallographic plane has been obtained in different peak (count) and angle positions (2θ). Initially, The plane for (101) is found approximated in the specific angle range 25.4^o-25.8^o and the peak shifted, such as shown in Fig. 2(a). Afterward the values 30.79^o-31.26^o for (102), the values 34.17^o-34.74^o for (211), the values 46.77^o-47.37^o for (311), the values 52.78^o-53.30^o for (222), and the values 59.41^o-60.06^o for (302), as shown all in Fig. 2(b)-2(f). These results indicated the rhombohedral structure of β-TCP nanopowders is formed with all peaks are shifted. Moreover, the PVA increased made each peak of the X-ray diffraction becomes optimum. Therefore, this would be affected the parameters of the crystallite size, crystallite strain,

crystallite dislocation, and crystallinity. Higher crystallinity value occurs for the sample 2.0 wt.% of PVA in approximated 77.66% and the lower value is 57.82% for the sample 1.0 wt.% of PVA, as shown in Table 1. When the peak of the X-ray diffraction is optimum and minimum the broad peak then its crystallinity tends to be high [18,25-26].
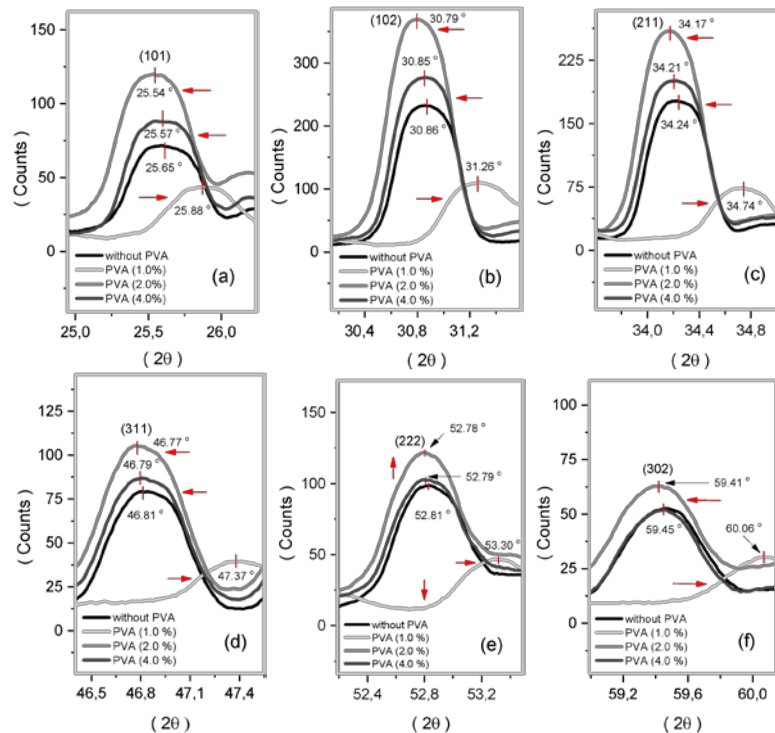

Fig. 2. X-ray diffraction patterns for β-TCP/PVA nanopowders with the Gaussian fit method in the specific region

The continued data analysis from XRD results by the approximated Gaussian fit method is used to describe the crystallography parameters of β-TCP nanopowders without or with the PVA effect. By using the Debye-Scherrer equation and Williamson-Hall plot method that are found the crystallite size, crystallite strain, and crystallite dislocation. The crystallite strain line curves for β-TCP nanopowders without PVA effect have been seen in Fig. 3(a) and Fig. 3(b)-3(d) for the crystallite strain line of β-TCP nanopowders with 1.0 wt%, 2.0 wt%, and 4.0 wt% of PVA, respectively. Whilst, in Fig. 3(e) is a straight line for crystallite strain compared to one another.

The considered standard equation of a straight line, the gradient or slope of Williamson-Hall plot is crystallite strain parameter (ε) and the y-intercept is Kλ/D. Which the parameters of K are numerical constant near unity, λ is wave-length of incident X-ray, and D is the average thickness of the crystal in a normal direction to the diffracting plane of *hkl,* and these parameters as described in the Debye-Scherrer equation. The crystallite size, crystallite strain, and crystallite dislocation values of β-TCP nanopowders without or with the PVA effect have been found by using the Eq. (6) to (7) and described in Table 1. The average of the crystallite size with small size occurs for β-TCP nanopowders with 1.0 wt% of PVA and the bigger size occurs for β-TCP nanopowders with 4.0 wt% of PVA. The crystallite size and crystallite strain both increases with PVA increase. Conversely, the crystallite dislocation tends to decrease, as shown in Table 1.
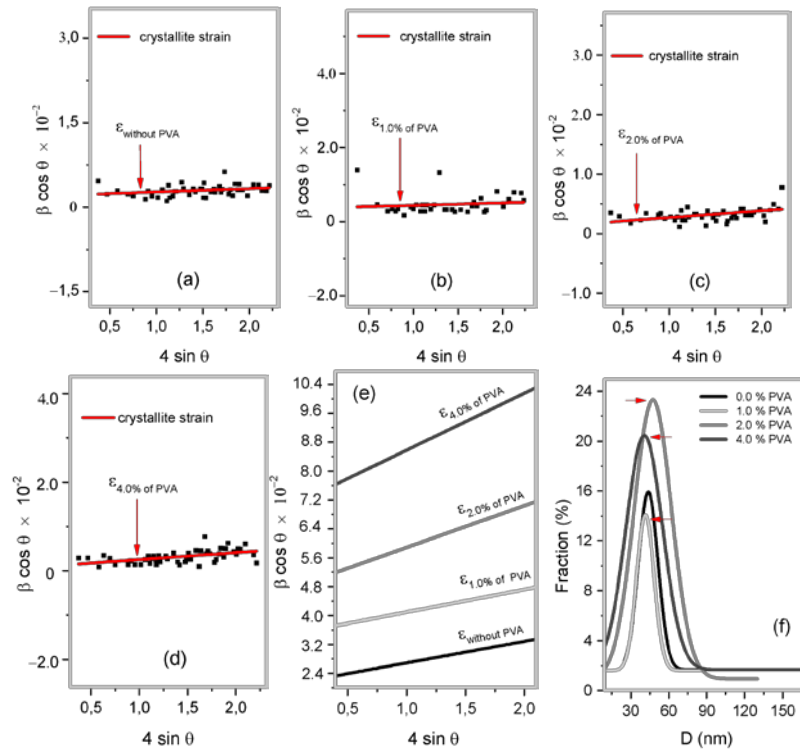
Fig. 3. The crystallite strain determination by the Gaussian fit method

The crystallinity degree or sometimes called the crystallinity of these samples has been defined by using the formulation such as in Eq. (11). This refers to the degree of structural order of solid material like a powdered crystalline. When the crystallinity is higher than lower values, it is meaning the structural order going to the long-range order than lower crystallinity. Many glass-ceramic and composite materials, can be prepared to produce a combination of the crystalline and amorphous regions.

$$Crystallinity = \frac{\text{Re } gion\, of\, crystalline\, peaks}{\text{Re } gion\, of\, all\, peaks\, (crystalline + amorphous)} \times 100\%. \tag{11}$$

The crystallinity of the sample with a higher value than the other was formed on the sample with 2.0 wt.% of PVA if it is compared to another sample such as 0.0 wt.% and 4.0 wt.% of PVA effect. In other words, the optimally of PVA to assists the crystallinity occurs in the value of 2.0 wt.% of PVA, such as shown in Table 1.

Table 1. The crystallite size average (D), crystallite strain (ε), and crystallite dislocation (δ), the crystallinity of β-TCP nanopowders without or with PVA effect

PVA (wt. %)	D (nm)	(ε ± Δε)	(δ ± Δ δ) (nm^{-2})	Crystallinity (%)
0.0	66.025	0.00063 ± 0.00031	0.0021 ± 0.00047	62.43
1.0	36.348	0.00059 ± 0.00095	0.0038 ± 0.00137	57.82
2.0	92.436	0.00181 ± 0.00034	0.0015 ± 0.00052	77.66
4.0	106.666	0.00194 ± 0.00039	0.0013 ± 0.00058	72.56

The crystallite size distribution of β-TCP nanopowders without or with PVA effect tend located in the range of 30 nm – 60 nm, as shown in Fig. 3(f). The crystallite size amount increase by increase the PVA, as shown in Fig. 4(a)-4(d). The localizing of the crystallite size in the ternary plot looks clear, which the sample without PVA has its crystallite size of 70 nm-100 nm, an amount between 0-25, and the fraction values obtained of 0%-25%. Whilst

for the sample with 1.0 wt% of PVA a lot found the crystallite size of 40 nm-70 nm, an amount between 30-60, and the fraction values of 25%-60%. Furthermore, for the sample with PVA of 2.0 wt%, a lot found its crystallite size of 20 nm-60 nm, an amount between 0-60, and the fraction values of 10%-40%. The last for the sample with 4.0 wt% of PVA, a lot found its crystallite size of 70nm-100 nm, an amount between 0-30, and the fraction value of 0%-25%.
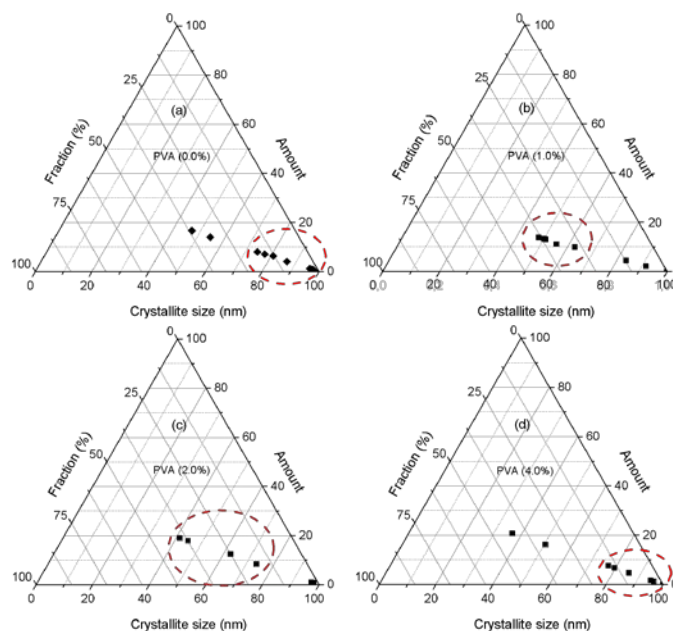

Fig. 4. Ternary plot of crystallite size for β-TCP/PVA nanopowders

DSC-TG results and discussion. Thermal analysis for β-TCP nanopowders without or with PVA effect for specific temperature and time through the determination of the fusion and crystallization enthalpies, melting point, and specific heat capacity has been conducted by using the DSC-TG result [27-28], as shown in Table 2 and Fig. 5. Previously, the DSC result described the heat flow as a function of temperature, as shown in Fig. 5(a). Where it describes the exothermic and endothermic processes so that values of the melting and crystallization are confirmed in Table 2 and Fig. 5(b). Afterward, the fusion and crystallization enthalpies described in Table 2. and Fig. 5(c)-5(d), which values of the enthalpies of fusion below and crystallization above the area, respectively. Whilst, the values of the initial and final melting point are both determined in Fig. 5(e) and its specific heat capacity determined in Fig. 5(f). This is compared just by two samples for β-TCP with 0.0 wt% and 4.0 wt% of PVA effect.

The DSC-TG examinations are conducted to only considered samples with 0.0 wt% and 4.0 wt% of PVA effect due to the presence of the without and higher influences in this research. Moreover, this examination for looking the primary data of effective temperatures to be compared by secondary data of effective temperature in the β-TCP/PVA nanopowder formation by sol-gel technique. Therefore, based on the comparative data of effective temperature by using the DSC-TG results in this research, such as shown in Table 2 with the secondary data obtained by several articles in the references, it was preferred to use effective temperature influence at ~ 800°C as a control variable in this β-TCP nanopowder with 0.0 wt% and 4.0 wt% of PVA effect.

As a comparison, all values of the fusion and crystallization enthalpies, melting point, and specific heat capacity for β-TCP nanopowders without and with 4.0 wt% of PVA are different, as shown in Table 2. This is indicated the PVA has been influenced by its thermal

response. Therefore, there are shifted peaks shown on the curves in Fig. 5. This data analysis of DSC result will be compared to the references using for temperature effect preferred in this research, such as 800°C.
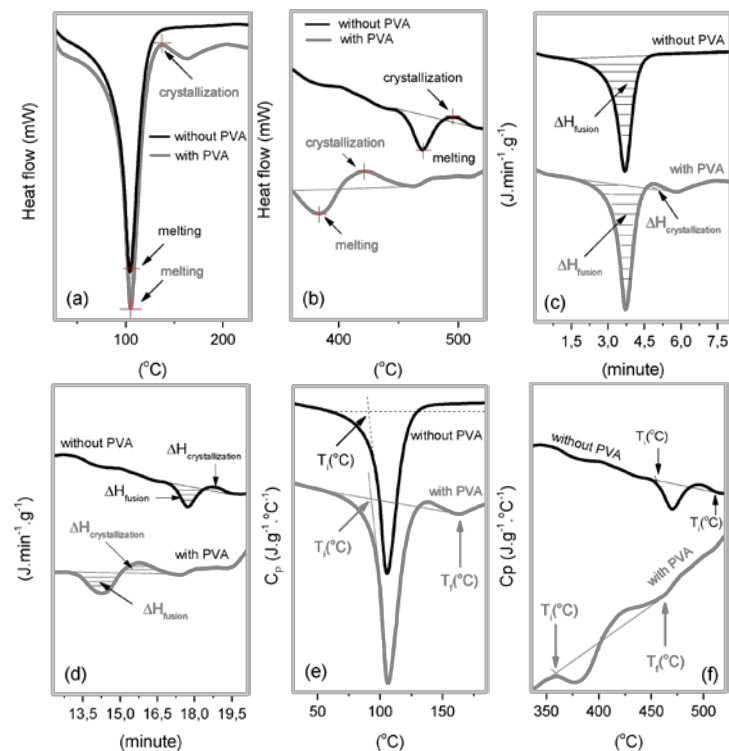

Fig. 5. The specific heat flow, melting point, specific heat capacity, fusion, and crystallization enthalpies are defined by using DSC curve analysis of β-TCP/PVA nanopowders

Table 2. The fusion and crystallization parameters of β-TCP/PVA nanopowders

Samples of β-TCP	Melting point range		Enthalpy of fusion	Enthalpy of Crystallization	Specific heat capacity
	$T_i(^oC)$	$T_f(^oC)$	$\Delta H_f(Jg^{-1})$	$\Delta H_C(Jg^{-1})$	$C_P(Jg^{-1o}C^{-1})$
.0 wt% of PVA	90.12	206	108.56	0.07	- 1.23
	225.26	265.88	3.08	0.19	0.37
	322.15	356.62	0.019	5.11	1.26
	456.52	513.64	30.73	6.66	0.09
4.0 wt% of PVA	90.14	132.05	1291.16	42.23	- 4.53
	361.47	466.64	58.66	27.47	- 0.62
	617.74	652.87	7.56	123.12	13.82
	939.26	961.54	8.97	11.54	6.23

     SEM-EDX results and discussion. SEM-EDX results for β-TCP nanopowders with 0.0 wt% and 4.0 wt% of PVA have been seen in Fig. 6(a) and Fig. 6(b). SEM result provides detailed images of the morphology [29], in which the surface topography of the sample with 4.0 wt% of PVA tends to be tight than the sample without or with 0.0 wt% of PVA. The results of the atomic ratio for β-TCP nanopowders with 0.0 wt% of PVA is Ca/P ≈ 1.62 and Ca/P ≈ 1.56 for β-TCP nanopowders with 4.0 wt% of PVA. The weight ratio is Ca/P ≈ 2.14 for β-TCP nanopowders with 0.0 wt% of PVA and Ca/P ≈ 2.26 for β-TCP nanopowders with 4.0 wt% of PVA.
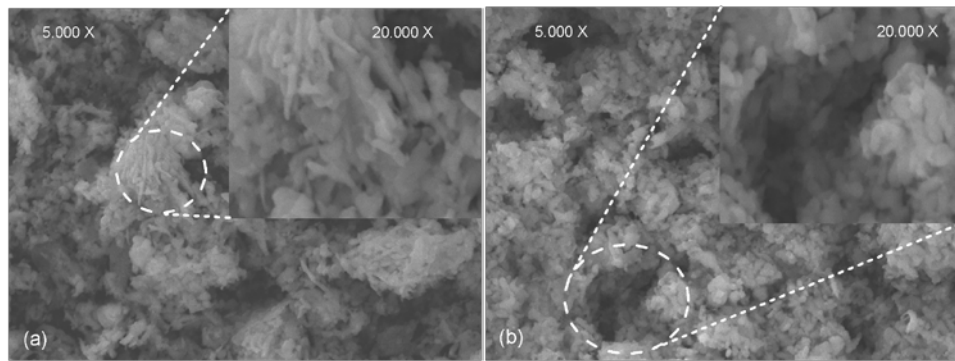
Fig. 6. SEM-EDX images for β-TCP/PVA nanopowders with; (a) 0.0 wt% and (b) 4.0 wt% of PVA

This quantity is compared by two samples for 0.0 wt% and 4.0 wt% of PVA of the formed of β-TCP nanopowders. Table 3. has been shown the element, weight, and atomic in the sample, which from its values of weight and an atomic ratio above have indicated to β-TCP nanopowders with 4.0 wt% of PVA a lot formed than the sample without or 0.0 wt% of PVA effect at specific heating of 800 ^{o}C. These samples are preferred to display by SEM-EDS test to look the differences between two samples without at 0.0 wt% and high value at 4.0 wt.% of PVA effect in this research.

Table 3. Quantitative of the element, weight, and atomic of β-TCP nanopowders with 0.0 wt% and 4.0 wt% of PVA samples

Samples of β-TCP	Element	Weight (%)	Atomic (%)	Error (%)
0.0 wt.% of PVA	O	47.94	68.27	10.81
	P	16.57	12.11	3.93
	Ca	35.49	19.62	3.13
4.0 wt.% of PVA	O	36.69	58.38	11.31
	P	19.43	16.26	3.61
	Ca	43.88	25.36	2.81

4. Conclusions

β-TCP/PVA nanopowders have been prepared by sol-gel technique at 800 ^{o}C with the preferential characteristics have found by the several interest parameters values determination. The Bravais lattice is found as a rhombohedral lattice system with fcc or ccp unit cell structure. Therefore, the rhombohedral lattice system was designed as β-TCP/PVA nanopowder and it was prepared by the sol-gel preparation technique in this research. Overall, the use of PVA has been contributed to achieving the nano-sized, crystallinity, and powdered of β-TCP/PVA. However, it is suggested to use this PVA in small amounts only to obtain the optimum values, such as found the optimum crystalline nano-sized at 1.0 wt.% of PVA and optimum crystallinity at 2.0 wt.% of PVA in this research.

The addition of PVA in the sol-gel technique of sample preparation for β-TCP/PVA nanopowders can be used as a novelty method in the fabrication, especially for biomaterial biocomposite of β-TCP nanopowders.

References

[1] Destainville A, Champion, Bernache-Assollant D, Laborde E. Synthesis, characterization and thermal behavior of apatitic tricalcium phosphate. *Material Chemistry and Physics.* 2003;80(1): 269-277.

[2] Liu B, Xing Lun D. Current application of β-tricalcium phosphate composites in orthopaedics. *Orthopaedic surgery.* 2012;4(3): 139-144.

[3] Reindl A, Borowsky R, Hein S, Geis-Gerstorfer J, Imgrund P, Petzoldt F. Degradation behavior of novel Fe/ß-TCP composites produced by powder injection molding for cortical bone replacement. *Journal of Materials Science.* 2014;49: 8234-8243.

[4] Liang L, Rulis P, Ching W. Mechanical properties, electronic structure and bonding of α- and β-tricalcium phosphates with surface characterization. *Acta Biomaterialia.* 2010;6(9): 3763-3771.

[5] Elliott J. Structure and chemistry of the apatites and other calcium orthophosphates: *Studies in inorganic chemistry.* Elsevier; 1994.

[6] Gibson I, Rehman I, Best S, Bonfield W. Characterization of the transformation from calcium-deficient apatite to β-tricalcium phosphate. *Journal of Materials Science: Materials in Medicine.* 2000;12: 799-804.

[7] Raynaud S, Champion E, Bernache-Assollant D, Thomas P. Calcium phosphate apatites with variable Ca/P atomic ratio I.Synthesis, characterisation and thermal stability of powders. *Biomaterials.* 2002;23(4): 1065-1072.

[8] Shadyah M.A, Nandakumar N, Joseph R, George K.E. On the facile polyvinyl alcohol assisted sol-gel synthesis of tetragonal zirconia nanopowder with mesoporous structure. *Advanced Powder Technology.* 2017;28(12): 3148-3157.

[9] Cernea M. Sol-gel synthesis and characterization of BaTiO3 powder. *Journal of Optoelectronics Advanced Materials.* 2005;7(6): 3015-3022.

[10] Ramesh S. Sol-Gel Synthesis and Characterization of Nanoparticles. *Journal of Nanoscience.* 2013: 1-8.

[11] Feng W, Mu-Sen L, Yu-Peng L, Yong-Xin Q. A simple sol-gel technique for preparing hydroxyapatite nanopowders. *Materials. Letters.* 2005;59(8-9): 916-919.

[12] Pereira M, Clark A, Hench L. Calcium phosphate formation on sol-gel-derived bioactive glasses in vitro. *Journal of Biomedical Materials Research.* 1994;28(6): 693-698.

[13] Ko E. Sol-Gel Process. In: *Preparation of Solid Catalysts.* WILEY-VCH; 2008. p.85-98.

[14] Znaidi L. Sol-gel-deposited ZnO thin films: A review. *Materials Science and Engineering B.* 2010;174(1-3): 18-30.

[15] Livage J, Sanchez C, Henry M, Doeuff S. The chemistry of the sol-gel process. *Solid State Ionics.* 1989;(32-33): 633-638.

[16] Hench L, West J. The sol-gel process. *Chemical Reviews.* 1990;90(1): 33-72.

[17] Owens GJ, Singh RK, Foroutan F, Alqaysi M, Han CM, Mahapatra C, Knowles JC. Sol-gel based materials for biomedical applications. *Progress in Materials Science.* 2016;77: 1-79.

[18] Patterson AL. The Scherrer formula for X-ray particle size determination. *Physical Review.* 1939;56(10): 978-982.

[19] Burton AW, Ong K, Rea T, Chan IY. On the estimation of average crystallite size of zeolites from the Scherrer equation: A critical evaluation of its application to zeolites with one-dimensional pore systems. *Microporous and Mesoporous Materials.* 2009;117(1-2): 75-90.

[20] Popa NC. The (hkl) dependence of diffraction-line broadening caused by strain and size for all Laue groups in rietveld refinement. *Journal of Applied Crystallography.* 1998;31(2): 176-180.

[21] Williamson G, Hall W. X-ray line broadening from filed aluminium and wolfram. *Acta*

Metallurgica. 1953;1(1): 22-31.

[22] Matěj Z, Kužel R, Nichtová L. XRD total pattern fitting applied to study of microstructure of TiO2 films. *Powder Diffraction*. 2010;25(02): 125-131.

[23] Ungár T, Borbély A. The effect of dislocation contrast on x-ray line broadening: A new approach to line profile analysis. *Applied Physics Letters*. 1996;69(21): 3173-3175.

[24] Epp J. X-ray diffraction (XRD) techniques for materials characterization. In: *Materials Characterization Using Nondestructive Evaluation (NDE) Methods*. Bremen, Germany; 2016. p.81-124.

[25] Groma I. X-ray line broadening due to an inhomogeneous dislocation distribution. *Physical Review B*. 1998;57(13): 7535-7542.

[26] Lindenmeyer PH, Hosemann R. Application of the theory of paracrystals to the crystal structure analysis of polyacrylonitrile. *Journal of Applied Physics*. 1963;34(1): 42-45.

[27] Menczel JD, Judovits L, Prime RB, Bair HE, Reading M, Swier S. Differential Scanning Calorimetry (DSC). *Thermal Analysis of Polymers: Fundamentals and Applications*. Wiley; 2008.

[28] Coats AW, Redfern JP. Thermogravimetric analysis. A review. *The Analyst*. 1963;88(1053): 906-920.

[29] McMullan D. Scanning electron microscopy 1928-1965. *Scanning*. 1995;17(3): 175-185.